Mat. Res. Soc. Symp. Proc. Vol. 746 © 2003 Materials Research Society

Precessional strategies for the ultrafast switching of soft and hard magnetic nanostructures

T. Devolder, M. Belmeguenai, H.W. Schumacher, C. Chappert, Y. Suzuki*.
Institut d'Electronique Fondamentale, UMR CNRS 8622,
Université Paris-Sud, 91405 Orsay, FRANCE.
*National Institute of Advanced Industrial Science and Technology,
Electronics Institute, Tsukuba, JAPAN.

ABSTRACT

We discuss the precessional, quasi-ballistic switching of magnetization in magnetic nanostructures. In soft spin-valve cells, fast and energy-cost effective magnetization switching can be triggered by a transverse field pulse of moderate amplitude, below the in plane anisotropy field, because of an amplification effect brought by the demagnetizing field at the early stage of the reversal. The same effect is no more possible in hard nanomagnets with perpendicular easy magnetization axis. We propose a new type of nanostructured magnetic device, designed to overcome this limitation. The speed is obtained through the use of a very high effective magnetic field, obtained by incorporating a significant exchange field which stores the energy in the form of a constrained domain wall surrounding a region of high magnetic anisotropy. This stored energy is partially available to accelerate the magnetization reversal in a precessional scenario. We illustrate the concept by studying numerically a model system. The key parameter for the reversal is the ratio of the domain wall width to the structure lateral dimension. Possible routes for device preparation are discussed. Promising application to magnetic storage are anticipated.

INTRODUCTION

Obtaining reproducible magnetization switching within the sub-nanosecond regime and the sub-micron range is currently one of the most challenging tasks in nanomagnetism. On the information storage front, it is of particular industrial interest to propose a writing strategy, which is fast, error-free in a large array of cells, energy cost-effective, and easily down-sizable. Both theoretical models [1] and time-resolved magneto-optic [2] or electrical [3] experiments can now account in details for the sub-nanosecond behavior of soft magnetic thin films and nanoelements. The magnetization dynamics is described by the Landau-Lifshitz equation [4] :

$$\frac{d\vec{M}}{dt} = \gamma_0 \vec{H}_{eff} \times \vec{M} - \frac{\alpha}{\|\vec{M}\|}\left[\frac{d\vec{M}}{dt} \times \vec{M}\right] \qquad (1)$$

where we use $\gamma_0 = -\gamma\mu_0$ instead of the classical gyromagnetic ratio γ. $\mathbf{H_{eff}}$ is the instantaneous effective field: $\vec{H}_{eff} = \vec{H} + \vec{H}_K + \vec{H}_{exch} + \vec{H}_D$. Here, $\mathbf{H}$ is the applied field, and $\mathbf{H_K}$ is the magnetocrystalline anisotropy field and depends on the relative orientation between the crystalline axes and the magnetization. The exchange field $\mathbf{H_{exch}}$ represents the energy stored in the magnetization torsion. The demagnetizing field $\mathbf{H_D}$=-$\mathbf{N.M}$, where $\mathbf{N}$ is the demagnetizing tensor, depends mainly on the relative orientation between magnetization and the principal axes of the magnetic element shape. We shall restrict below to the case of flat nearly elliptical platelets, elongated along x, where we have the relation $N_x \leq N_y << N_z \approx 1$.

The time evolution scales with the Uniform Precession (UP) frequency $f_{UP} = (\gamma_0/2\pi)\, H_{eff}$, where $-\gamma/2\pi = 28$ GHz/T. The relaxation towards equilibrium is described phenomenologically

by the damping constant α, with $1/\alpha\gamma_0 H_{eff}$, typically about 0.2-2 ns, characterizing the energy relaxation time. In the following, we affect the symbol "°" to zero applied field quantities.

The conventional strategy to reverse magnetization is to apply an external field **H** antiparallel to the equilibrium magnetization. This strategy remains efficient in quasi-static reversal, when thermal activation helps to overcome the energy barriers [5]. In the ultrafast limit, a step of external field applied roughly antiparallel to **M** makes it undergo multiple precessions about the local effective field before reaching full reversal ([2,3]). The resulting reversal times are thus much longer than the precession period.

The non-conventional ultrafast magnetization reversal strategies can be classified in two categories : (i) for magnetically soft material where the equilibrium effective field is almost zero or (ii) for magnetically hard material, where the equilibrium effective field can be huge. We shall in the following discuss two model configurations:

(i) *In soft in plane magnetized elements*, the effective field $\mathbf{H}_{eff}$ is nearly zero when magnetization **M** is at rest along its equilibrium axis. To achieve fast reversal, the external field **H** creates a significant additional perpendicular demagnetizing field that drives the motion of the magnetization through the torque $\mathbf{H_D}$x**M**. The most striking application of this strategy is the so-called precessionnal switching [6-9] of soft elements, for which a magnetic field pulse is applied along the short axis of a soft platelet. The reversal lasts only typically few times $1/\gamma_0\sqrt{2H.M_S}$, and can be as small as 150 ps (section I).

(ii) *In hard perpendicularly magnetized elements*, the effective field incorporates the anisotropy field and can thus be huge at equilibrium, when $\mathbf{H}_{eff}°$ and **M**° are collinear. In consequence, to achieve reversal the applied field must first create a significant angle between the effective field $\mathbf{H}_{eff}°$ and a displaced magnetization. To achieve cost-effective reversal, we propose that the external field is immediately relayed by a strong "helping" field with a *different symmetry* from the anisotropy field. The required helping field magnitude is typically $(H_K-M_S)/2$, and may be of exchange origin. Switching speeds below 150 ps may then be obtained. We propose a practical device, where the exchange field can be stored in the form of a domain wall surrounding a small, high magnetic anisotropy region (Section II). To access the real technological potential of the concept, we numerically study a model sample, that could for instance be realized by using local light ion irradiation techniques [10]. First attempts to fabricate such a device are reported.

I. PRECESSIONAL REVERSAL IN SOFT MAGNETIC MATERIALS

In this section we deal with soft magnetic materials. In related devices, $\mu_0\mathbf{H}_K$ and the in plane shape anisotropy $(N_y-N_x)\mathbf{M}_s$ are of the same order of magnitude and can be included in a total anisotropy field $\mu_0\mathbf{H}_A$ of order typically a few mT. We will also assume a coherent reversal (M stays uniform), and so H_{exch} will be neglected.

I.A. Precessional reversal strategy in soft systems

For an efficient magnetization reversal scheme, the initial torque $\mathbf{H}_{eff}$ x **M** should be near maximum, and so the external field should be applied at an angle $\pi/2$ with respect to the magnetization.

The resulting magnetization reversal precessional scenario [11,12] in a soft rectangular platelet is depicted in Figure 1. The field pulse **H** is applied along the short (hard) axis of the platelet (step 1). This initial torque pushes the magnetization out of the film plane at a rate $\gamma_0 M_S H$. The resulting demagnetizing field grows during a given settling time τ_1 (step 2 of Fig.1).

After this delay τ_1, the demagnetizing torque gets greater than the Zeemann torque and magnetization precesses then mainly around the demagnetizing field, perpendicular to the platelet (step 3 of Figure 1). This induces a 180 degrees reversal of the magnetization of duration τ_2. If the magnetic field is switched off at the particular time $\tau_1+\tau_2$, magnetization falls into the nearest energy minimum, which has a reversed magnetization.

I.B. Experimental results on soft, micron-sized spin valve cells

This precessional strategy has been tested by H. W. Schumacher et al. [7,9] on stadium shaped 5µm x 2.3µm spin-valve cells. The soft layer is CoFe 20 Å / NiFe 30 Å. The total in plane anisotropy field of that element is H_A~ 7.5 mT. The transverse field pulse is generated by a current pulse injected into a buried high bandwidth coplanar line, while magnetization reversal is followed by magneto-resistance using a 40 GHz bandwidth electrical set-up [13].

A representative time-resolved measurement of the magnetization switching process in that soft cell is displayed on Figure 2. The 165 ps transverse pulsed field reaches 8 mT with rise time 45 ps (Fig.2B). Fig.2A is a macrospin simulation assuming a sample with diagonal demagnetizing tensor. Fig.2C is the experimental magneto-resistive response of the spin-valve. The 20%-80% reversal takes places in a time interval of 130 ps. As shown in [7], such precessional scenario can be obtained at applied fields below the Stoner-Wohlfarth scenario.

I.C. Discussion

We first estimate the time needed for the full switching of a soft cell, when using a precessional strategy. We then comment on the requirements on the magnitude of the applied field by comparison to the Stoner-Wohlfarth mechanism. A comprehensive discussion of the requirements on the field pulse duration can be found in ref. [7]. Also, we will assume here $H>>H_A$: a more detailed treatment of the influence of H_A is beyond the scope of this paper.

1. Analytical estimate of the switching time

We assume $H << M_S$ and $\alpha << 1$ (energy conservation). We note ϕ the angle between **M** and the platelet plane (xy). **H** creates an initial torque which pushes **M** out of the film plane as :

$$dM_z = \gamma_0 \, H.M_x(t).dt \qquad (2)$$

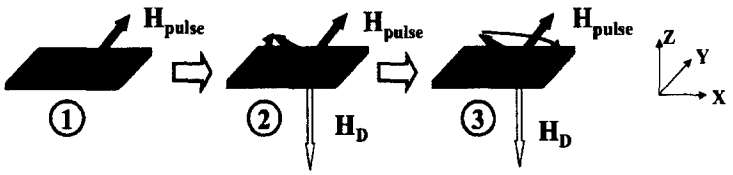

Figure 1 : Sketch of the precessional switching scenario on a soft platelet. At step 1, a hard axis field pulse is applied onto the platelet of initial magnetization (black arrow) along the easy axis. At step 2, magnetization is lifted out of the film plane, thus creating a strong out-of-plane negative demagnetizing field. Magnetization precesses about this demagnetizing field and proceeds to a 180° reversal (step 3).

This results in a demagnetizing field growing approximately as $-\gamma_0 H.M_S.t.z$. Eq.1 projected on the (y) axis leads to a quadratic dependence of M_y at small t. The initial evolution of M_x is found by projecting Eq.1 on the (x) axis and keeping the terms of lowest order in time dependence. M_x evolves quadratically with time as :

$$M_x(t) - M^\circ_x \approx \tfrac{1}{2} \gamma_0^2 M_S.H^2.t^2. \qquad (3)$$

During this regime, the projection of **M**(t) on the easy axis will not change much. This appears to experimentalists as a delay τ_1 before reversal effectively starts.

After this delay τ_1, the demagnetizing torque exceeds the Zeemann torque and magnetization precesses then mainly around the demagnetizing field. This induces the 180 degrees reversal lasting τ_2.

To estimate τ_2, we focus on the particular instant when **M** is above the hard axis, i.e. between step 2 and 3 of Figure 1. We have $M_x=0$, $M_y = M_S.\cos\phi$ and $M_z = M_S.\sin\phi$. At that time, the initial Zeemann energy $\mu_0 \mathbf{H}.\mathbf{M}_{(t=0)}=0$ has decreased to $-\mu_0 HM_S \cos\phi$, and has almost entirely flown into the demagnetizing energy. We thus can write :

$$\mu_0 HM_S \cos\phi = \tfrac{1}{2} \mu_0 M_S^2 \sin^2\phi. \qquad (4)$$

Since $H << M_S$, the angle ϕ is weak, and $\sin\varphi \approx \sqrt{2H/M_S}$. Around this instant the precession frequency is approximately $(\gamma_0 H_D/2\pi)$, and the characteristic switching time τ_2 can be evaluated from this frequency:

$$\tau_2 = \left(\pi / \gamma_0 \sqrt{2H.M_S} \right) \qquad (5)$$

The initial delay τ_1 is about the time it takes for $\mathbf{H_D}$ to settle its magnitude and start switching the magnetization. In the linear approximation of Eq. 2, this time is passed when M_z reaches its maximum $\sqrt{2H.M_S}$, and so we can evaluate τ_1 as:

$$\tau_1 \approx \left(2 / \gamma_0 \sqrt{2H.M_S} \right) \qquad (6)$$

It follows immediately that the characteristic total reversal time will scales with: $1/\gamma_0\sqrt{H.M_S}$.

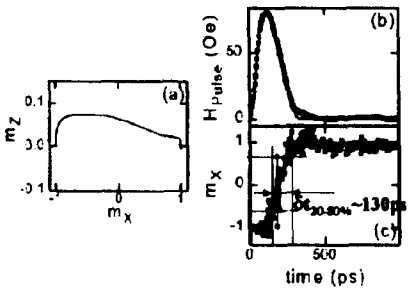

Figure 2 (courtesy of H.W. Schumacher, C. Chappert, R.C. Sousa, P.P. Freitas and J. Miltat, [9]). (A): Macrospin calculation of the precessional switching trajectory in the XZ plane. The field pulse is stopped after a 180° precession about H. (B): Experimental field pulse of 8 mT and 165ps duration. (C): Normalized experimental Magneto-resistive response of the spin-valve (gray dots) and simulation (full line) of the easy axis component of the magnetization.

The previous approach focused on the initial stages of the magnetization reversal. It is worth completing this approach by studying magnetization fluctuations long after the onset of the external field, which we now assume to be a Heavyside step function. In our hypothesis that $H>H_A$, the final magnetization lies along the in-plane hard axis. As a result, **H** is transverse to **M** at t=0 and longitudinal at $t\rightarrow\infty$.

Classical Ferromagnetic Resonance (FMR) theory [14] indicates that the long term uniform precession (UP) mode is about the applied field, with a frequency $\omega_{UP} = \gamma_0\sqrt{(H-H_A)(H+(N_z-N_y)M_S)} \approx \gamma_0\sqrt{H.M_S}$, and that this UP mode can be efficiently pumped at $t = 0^+$ because the initial field is transverse.

Hence the long-term characteristic FMR frequency and our estimated switching frequency both scale with $\gamma_0\sqrt{H.M_S}$, which further confirms our evaluation.

2. Minimal cost in applied field

Stoner-Wohlfarth switching theory [15] assumes coherent rotation and zero temperature, and derives switching fields H_S from the *sole* criteria of energy local minimum. This gives the well know asteroid curve when plotting the orientation dependence of H_S in the plane of the samples.

Although the precessional switching is also a coherent behavior, it would be wrong to assume the same orientation dependence for the switching fields. The reason is that, while in Stoner-Wohlfart analysis the field is sweep *slowly*, such that the energy dissipation is *always* fast enough to stabilize magnetization in the nearest energy minimum, in the precessional strategy, the field is swept very rapidly and magnetization is *never* in an energy local minimum after t=0.

In the geometry described in this paper, with H greater than the anisotropy field H_A, there exists *only one* equilibrium magnetization orientation, along **H**. As a result, the magnetization trajectory is almost symmetric around **H** (in the case $\alpha<<1$), and the applied field pulse length must be fitted to odd multiples of the switching time to achieve reversal [7, 16]. Ballistic, non-ringing trajectories require to stop the applied field exactly when $M_z(t)=0$ [7, 9, 17].

The situation is more complex when H is smaller than the anisotropy field H_A., because there exists *two* degenerate stable magnetization orientations. The final state will thus depends on the history and can not be derived from sole energy considerations. Field pulse rise time and length must be precisely controlled, and switching can be obtained at fields lower than Stoner-Wohlfarth switching fields [12, 16]. For instance, G. Albuquerque et al. [17] have extended this analysis and shown that, in the limit of vanishing α and infinitely small rise-time, a transverse field of $H=H_A/2$, i.e. half of the Stoner-Wohlfarth switching field, is enough to trigger magnetization switching. The work of H.W. Schumacher et al. ([7, 9]) is to our knowledge the first experimental demonstration of such precessional, sub Stoner-Wohlfarth switching.

One important criterium must finally be discussed. Achieving the excitation of a precession mode requires the excitation field time dependence to comprise Fourrier components of frequencies above the precession characteristic frequency. Success of the precessional strategy thus requires:

$$1/H\ (dH/dt) >> \gamma_0\sqrt{H.M_S} \qquad (7)$$

In the experiments described in § I.B (Figure 2), precession effects strongly dominate since $1/H\ (dH/dt) \approx 20$ GHz and $\gamma_0\sqrt{H.M_S} \approx 3$ GHz.

II. PRECESSIONAL REVERSAL IN HIGH ANISOTROPY SYSTEMS

Two terms have been ignored so far in the Landau-Lifshitz equation: the magneto-crystalline anisotropy and exchange fields. In this section, hard material nanostructures are considered, and $\mathbf{H_K} = H_K \mathbf{z}$ is assumed to be higher than M_S. The effective perpendicular anisotropy H_K-M_S is typically 0.1 to 1 T. $\mathbf{H_{exch}}$ will be introduced in §II.C.

II.A. Adapting precessional strategy to high anisotropy systems

The uniform FMR mode of a soft platelet around the stable equilibrium position in zero applied field is given by $\omega_{UP} \approx \gamma_0 \sqrt{M_S H_A}$ [14], where H_A is small. The UP trajectory is very elliptical : the in-plane aperture angle is much greater than the out-of-plane angle. This provides a path for reversing the magnetization through a quasi easy-plane trajectory (section I).

The situation is very different for a hard platelet with high perpendicular anisotropy. The UP frequency in zero applied field is $\omega_{UP} = \gamma_0 (H_K - M_S)$, such that the intrinsic dynamics of the system is already faster than for a soft platelet (by a factor of about 2 with the parameters of this paper). But, as (H_K-M_S) is much greater than any in plane anisotropies, the UP trajectory is nearly circular around the anisotropy axis, which does not provide an easy path for reversal. Considerably much higher transverse fields are required to pump these modes compared to a soft material. Following the arguments of § I.C.2, and considering that hard materials usually experience high damping, reversing the magnetization requires fields of the order of (H_K-M_S).

Circumventing this difficulty requires to *favor* the pumping of *only one* transverse magnetization component to make the UP much more elliptical. This may be done by adding an additional term in the effective field, with a *different symmetry* from that of the anisotropy field. In the next subsection, we consider such an extra $\mathbf{H_X}$ field in the (x) direction, with typical strength $\mu_0(H_K$-$M_S)/2$. In section II.C we will propose to use an exchange field $\mathbf{H_{exch}}$ for this purpose. More general considerations on speed and energy cost will be given in section II.D.

II.B. Precessional reversal strategy in hard systems

Let us consider the state defined in step 1 of fig.3. The magnetization at rest (black arrow in Fig.3) is parallel to the effective field, i.e. the vector sum of an extra field $\mathbf{H_X}$ along (x), an anisotropy field along (z) and a demagnetizing field along (-z).

To induce magnetization reversal, the external field **H** (gray arrow in fig.3) is applied along the (x) direction. The Zeemann torque extracts **M** from the (xz) plane at a rate $\gamma_0 M_S.H.\sin\phi$ (step 2). Precession is initiated and **M** is sent towards the (xy) plane. The effective anisotropy field ($\mathbf{H_K}$-$\mathbf{M_z}$) decreases as M_z as **M** approaches the film plane. At step 3, magnetization is in the (xy) plane: ($\mathbf{H_K}$-$\mathbf{M_z}$) vanishes and the precession proceeds around ($\mathbf{H_X}$+**H**). However, the movement of **M** slows down. The applied field can be possibly stopped at step 3: the *sole* extra field can finish the job until step 4, when M_z is strongly negative, and the anisotropy field has reset and stabilizes **M** to a "reversed" position. However the movement is faster if the field **H** is not switched off at step 3.

II.C. Micromagnetic illustration of the concept

One way to reach high enough values for this extra in-plane field H_X is to use exchange energy. This can be done for example by depositing a high perpendicular anisotropy alloy onto an antiferromagnetic buffer creating an in-plane exchange bias. In that case, the exchange field can reach typically 250 mT [18], which would be sufficient for our goal.

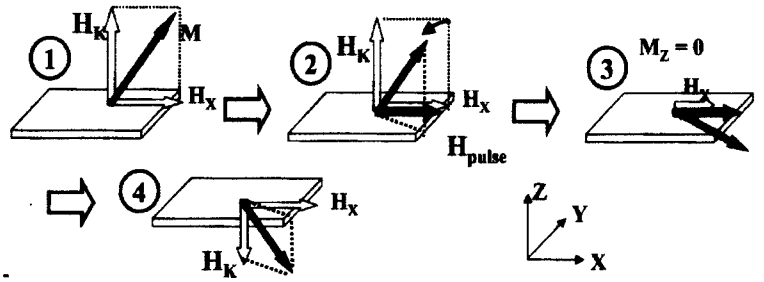

Figure 3 : Sketch of the precessional switching scenario of a hard platelet with perpendicular anisotropy subjected to an in-plane exchange field. Step 1: equilibrium configuration: **M** is in the (xz) plane, making an angle ϕ with the (xy) plane. An extra field $\mathbf{H_X}$ lies along (x). Step 2: an in-plane field pulse parallel to $\mathbf{H_X}$ tilts the magnetization out of the (xz) plane. Magnetization starts to precess about the effective field. Step 3: if the $\mathbf{H_X}$ torque exceeds the anisotropy torque, magnetization proceeds with a precession around $\mathbf{H_X}$+**H**. The applied field can be switched off as soon as **M** crosses the xy plane. At $M_z(t)=0$, the sole $\mathbf{H_X}$ torque exists and pushes M further under the (xy) plane, while the anisotropy field resets to stabilize **M** at an angle $-\phi$ with respect to (z).

Such a high exchange field can also be found in a strong magnetization gradient. This occurs for instance in a Bloch domain wall, where the local exchange torque is of the order of the effective anisotropy torque. In the following, we will address this configuration.

Let us give an example of how a precessional strategy could be implemented on a nanostructure of perpendicular anisotropy, with non-uniform magnetization at equilibrium. In the Fig. 4 and 5, we report the calculated time evolution of <**M**> in a system comprising a high anisotropy central nanostructure surrounded by a peripheral zone (the "matrix") of weaker anisotropy. The fabrication of such a device will be discussed in §II.E.

The central 128x64 nm² area possesses a high perpendicular anisotropy ($K=1.45\times10^6$ J/m³, $\mu_0(H_K-M_S)=250$ mT) while the complement of the 256x128 nm² rectangle (the matrix) has a smaller anisotropy ($K=7.25\times10^5$ J/m³, $(\mu_0(H_K-M_S)=-770$ mT). Magnetization is everywhere $\mu_0 M_S=1.79$ T. The easy axis is thus perpendicular to the film plane in the center of the cell, whereas shape anisotropy dominates in the surrounding matrix. The rectangular shape creates a S-like state [11] with an in-plane remanence mainly along the easy axis (Figure 5A). A domain wall separates the central part and the matrix. Because the matrix and the central part are exchange coupled through this wall, the central part feels an in-plane exchange field, which slightly tilts its magnetization away from the magneto-crystalline anisotropy axis (z). With the parameters above the tilt angle is only 11deg. in the center.

We assume a film thickness of 14Å, a damping constant $\alpha=0.2$ [19], and an exchange stiffness of 3×10^{11} J/m. Such parameters are compatible with those of Pt/Co/Pt sandwiches. At $t = 0^+$, a 150 mT field step is applied along the long axis (x) of the platelet. This field is parallel to the magnetization of the matrix, such that **M** will not evolve much in the matrix.

On the contrary, the precession induced by the Zeeman torque inside the central zone extracts its magnetization out of the (xz) plane.

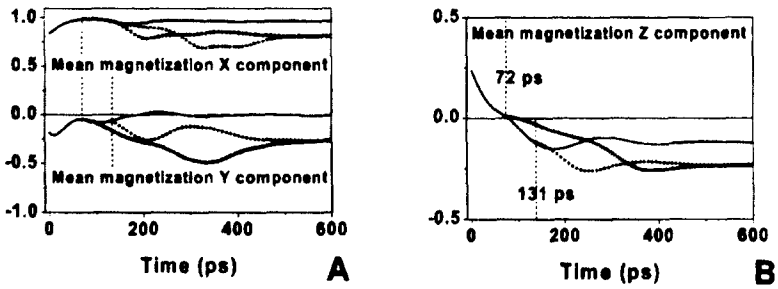

Figure 4 : Micromagnetic simulation of the precessional switching trajectory of a system comprising a 128x64 nm² high anisotropy ($K=1.45\times10^6$ J/m^3) nanostructure embedded in the middle of a 256x128 nm² rectangle platelet with half anisotropy. Saturation magnetization is 1.79 T, film thickness is 1.4 nm. (A): X and Y components of the mean magnetization. (B): Z component of the mean magnetization The 150 mT field pulse is stopped at 72 ps (after a 90° precession) in the curves with cross points, at 131 ps (after a 180° precession) in the curves with circular points, and is never stopped in the full line curves.

M_y grows first (Figure 5B) at the expense of M_z, and then the precession sends **M** towards the platelet plane. At t=72 ps, the mean magnetization lies in the platelet plane (Figure 4): M has undergone a $\pi/2$ precession around the (x) axis. The precession is quicker in the domain wall, where the exchange torque is maximum, such that the z-component reverses first near the initial domain wall position (Figure 5C). This is further favored at the left and right domain walls surrounding the central part because there, an extra in-plane dipolar field along (x) is (constantly) generated by the matrix.

At t=72 ps, the anisotropy field is zero, such that the precession speed comes solely from the weak external field and the exchange field. Note that this exchange field comes only from the y-component of **M** and so is weaker than initially. This slows down the magnetization evolution, which corresponds to the inflexion point at $\langle M_z(t)\rangle=0$ (Figure 4B, t = 72 ps, full line curve).

Three scenarii can then be chosen:

(i) If the external field is maintained, the magnetization in the central part has fully switched after 131 ps (Figure 5D). A small ringing persists for some 100 ps longer (Figure 4), and the final state in constant applied field has negative M_z component, but M_y is zero (Figure 5E). If the field is removed at t >> 1 ns (not shown), the system may evolve to any of the two S-states (M_y positive of negative) that are degenerate in energy. A crucial point is that the applied field is not strong enough to force the magnetization of the central part of the structure to be in the plane. This means that, as for the soft elements, switching can be obtained with fields *smaller* than the one obtained for a Stoner-Wohlfarth switching mechanism, at least within our scheme.

(ii) The post-reversal ringing can be avoided if the field is switched off at t = 131 ps, i.e. after a π precession about the (x) axis. In that case, the pulse duration is matched to the first harmonic of the switching characteristic frequency, and ballistic switching is achieved. The final S-state of the matrix has the same chirality as the initial S-state, so the reversal is reversible.

(iii) In fact, the applied field can be already switched off at $\langle M_z(t)\rangle=0$, i.e. at t = 72 ps. The precession about the (x)-axis continues, but the torque is solely due to the exchange field,

which is reduced compared to its initial value. The long-term ($t \geq 500$ ps) equilibrium state is the reversed magnetization state in the central high anisotropy area, and the initial S-state in the matrix. Meanwhile, a significant ringing of M_x and M_y is present (Figure 5F) during the slow, more regular evolution of M_z towards the reversed equilibrium state ($M_z<0$).

II.D. Discussion

As formerly done for the soft elements, basic analytical considerations can give some useful insight into the critical parameters.

1. Requirements on the equilibrium exchange field

Let's first discuss the configuration of Fig.3. The field pushes initially (as $t << 1/\gamma_0 H$) the magnetization out of the film plane at a rate $M_y(t) = \gamma M_S.H.\sin\phi\ t$ (step 2 of Fig.3). Then, the effective field bents this movement. The projections of Eq.1 on the (x) and (z) axes give:

$$M_z(t) - M^\circ_z = -\tfrac{1}{2}\gamma_0^2 M_S.H.\ t^2.(H+H_X).\sin\phi \qquad (8)$$

$$M_x(t) - M^\circ_x = \tfrac{1}{2}\gamma_0^2 M_S.H.\ t^2.(H_K-M_S).\sin\phi \qquad (9)$$

In order to initiate a precession around (x), and not (z), we need to have: $(M^\circ_z - M_z(t)) > (M^\circ_x - M_x(t))$, i.e. $(H+H_X) >> (H_K-M_S)$. So precessional switching may be achieved for moderate field H only if much energy is stored in H_X, i.e. in the exchange energy.

In the geometry of figure 3, the best compromise between large M_z signal (e.g. for a recording application), and cost in applied field H, is thus near $H_X \approx (H_K - M_S)/2$, which gives a tilt angle ϕ° at rest around 45 degrees. This is exactly the order of magnitude of H_X that we had proposed without justification in §II-A and §II-B.

For the configuration of figure 5 and §II-C, the condition equivalent to $H+H_X \geq (H_K-M_S)$ at moderate fields H is that the central area should not be much greater than the Bloch domain wall width, where exchange energy is stored. This is the case with our parameters, and one advantage of this geometry compared to that of figure 3 is that the central part can still remain nearly perpendicularly magnetized at rest. However, the reversal will be initially more efficient inside the domain wall (see Figure 5C), where the exchange field is maximal.

2. Conjecture on the switching time

In contrast to soft systems (I.C.1), an analytical estimate of switching time for high anisotropy systems may not be derived from simple energy considerations. The energy loss rate is too high in hard materials for energy conservation considerations to reasonably apply.

In addition, the remaining part of the initial Zeemann energy does not flow solely in the exchange energy but rather shares itself towards exchange and anisotropy energies, such that the exchange torque when $M_z(t)=0$ may only be calculated through full micromagnetic simulations.

As done in §I.C.1, it is worth studying magnetization fluctuations around the micromagnetic state of Figure 5E, i.e. long after the onset of a Heavyside step external field satisfying $H+H_X > H_K-M_S$ and thus aligning the magnetization in the (x) direction.

Again, the long term UP mode has a frequency which scales roughly with $\gamma_0\sqrt{(H+H_X-(H_K-M_S))(H+H_X)}$ or equivalently $\gamma_0\sqrt{(H-(H_K-M_S)/2)(H_K-M_S)}$, for the optimal "signal to speed" compromise. We anticipate that the characteristic reversal time is related to the latter frequency. Further calculations are in progress to confirm this point.

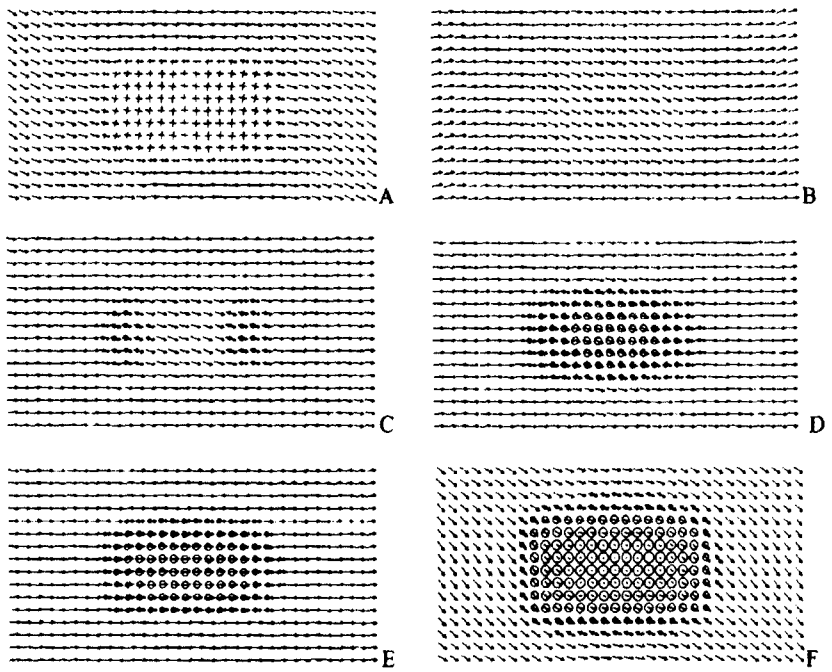

Figure 5 : Snapshots of the time-evolution of magnetization during precessional switching of the nanostructure defined in the text. The arrows stand for in the in-plane magnetization. The circles or the crosses have sizes proportional to the out-of-plane (z) component of the magnetization (crosses for $M_z > 0$). (A) is the equilibrium state: the central, high anisotropy area has upwards perpendicular magnetization. The surrounding's magnetization points to the right. An in-plane 150 mT field along the long axis of the cell is applied on state A. States B, C, D and E are respectively snapshots after 60 ps, 72 ps, ($\pi/2$ precession angle), 132 ps (π precession angle) and 1 ns (equilibrium state in constant applied field). State F is the relaxed state after 300 ps, obtained if the field is suppressed 72 ps after its onset.

II.E. Possible fabrication routes

One way to fabricate the nanostructure of Figure 5A is to use light ion irradiation patterning [10] on a system with initial perpendicular anisotropy. For instance, 30 keV He^+ ion irradiation of Co-Pt multilayers with perpendicular magnetization easy axis was shown to be a powerful tool to tune their magnetic anisotropy. In these materials, ion-mixing at the Co/Pt interfaces gradually reduces the magnetic anisotropy energy in a controlled way, which first lowers the coercive force, then triggers an in-plane reorientation of the magnetization easy axis. Embedded hard magnetic nanostructures as small as 30 nm were demonstrated when the irradiation is performed through a mask directly patterned on the sample surface [20].

Figure 6 : Optical micrographs of prototype devices designed for broadband measurements of the precessional switching of a nanostructure with perpendicular anisotropy. (A) global 2x1.5 mm² view of the circuit. (B) Zoomed 200x150μm² image: magnetic Hall cross with 500 nm wide arms located above the 4μm wide stripeline used to generate the field pulse. The faintly visible 100x100μm² square is a silica layer isolating the Hall cross from the pulse line.

One weakness of this approach is the intrinsically non-abrupt character of the transition between in plane and perpendicular magnetized areas. The transition width is comparable to a domain wall width, which will reduce the amount of exchange energy stored. Potentially more abrupt anisotropy transitions may be obtained following the technique developed in ref. [21]. The technology to fabricate the device studied in §II.C is thus certainly available.

Prototype devices are shown in Figure 6. The nanostructure will be irradiation-fabricated at the center of a Hall cross structure (Figure 6B), contacted to 4 coplanar stripes designed for Extraordinary Hall Effect measurement. The Hall cross is a Co/Pt multilayer with perpendicular magnetic anisotropy. The diagonal arms serve as DC current injection arms while the 50 μm wide vertical arms are 50 Ω coplanar waveguides that serve for the high frequency Hall voltage measurement. This cross is located above another 4μm wide coplanar waveguide that generates the fast rising in-plane magnetic field pulse. This pulse line is electrically isolated from the magnetic Hall cross by a silica layer (Figure 6B). First electrical characterizations indicate sufficient signal/noise ratio for high frequency magnetization dynamics measurement.

CONCLUSION

Through the derivation of approximate analytical expressions we have discussed the precessional switching of magnetization in soft and hard (perpendicularly magnetized) nanoplatelets. Fast, energy cost-efficient precessional switching was recently demonstrated in soft platelets [9, 11], and a similar result for hard platelets would be of high interest for application to for instance perpendicular hard disk recording. It may also become a crucial issue for the future of M-RAM technology, when largely sub-100 nm sizes will require high magnetic anisotropy to ensure thermal stability.

The main differences between soft and hard platelets lies in their damping coefficient α, and their effective field $H°_{eff}$ near the stable equilibrium position. In soft platelets, α and $H°_{eff}$ are weak, and $H°_{eff}$ furthermore shows a strong easy plane symmetry. This enables fast (~150 ps) precessional reversal in moderate in-plane transverse applied fields.

On the contrary, hard platelets exhibit strong $H°_{eff}$, with nearly cylindrical symmetry around the perpendicular axis, together with a strong damping. So pumping of precessional modes will require high in-plane fields. We have shown that it is possible to bend this issue by adding and extra in-plane field H_X that breaks the cylindrical symmetry of $H°_{eff}$. We have further shown that H_X can be of exchange origin, and proposed a numerical example of realization, that

could be experimentally implemented. High reversal speeds can be expected, at fields as low as half of the perpendicular anisotropy field.

However, although in this paper we have restricted our discussion to exchange fields, we want to stress that the main concept of breaking the circular symmetry of a strong perpendicular anisotropy, in order to enable precessional switching in moderate in plane fields, holds a much more general validity. A similar effect could be obtained for instance with a tilted anisotropy axis, although analytical expressions would be slightly different because of the different dependences in M orientation for Zeeman and anisotropy energies. A more elaborate treatment of these effects will be published in a forthcoming paper.

ACKNOWLEDGEMENTS:

The authors wish to thank Jacques Miltat and Harry Bernas for enlighting discussions. The work was supported in part by the NEDO contract "Nanopatterned magnets".

REFERENCES

1. *Spin Dynamics in Confined Magnetic Structures*, B. Hillebrands and K. Ounadjela (Springer, Berlin, 2001).
2. B. C. Choi et al., *Phys. Rev. Lett.* **86**, 728 (2001) ; W. K. Hiebert, G. E. Ballentine, and M. R. Freeman, *Phys. Rev. B* **65**, 140404(R) (2002)
3. R. H. Koch et al., *Phys. Rev. Lett.* **81**, 4512 (1998)
4. L. Landau, E. Lifshitz, *Phys. Z Sowjetunion* **8**, 153 (1953); T.L. Gilbert, *Phys. Rev.* **100**, 1243 (1955).
5. *"Classical and quantum magnetization reversal studied in nanometer-sized particles and clusters"*, W. Wernsdorfer. To be publ. in *Advances in Chemical Physics* (Wiley Ed.), 2003.
6. Th. Gerrits, H. A. M. Van Den Berg, J. Hohlfeld, L. Bär, Th. Rasing, *Nat.* **418**, 6897 (2002)
7. H.W. Schumacher, C. Chappert, P. Crozat, R. C. Sousa, P. P. Freitas, J. Miltat, J. Fassbender, and B. Hillebrands, *Phys. Rev. Lett.* **90**(1), 017201 (2003).
8. S. Kaka and S. E. Russek, *Appl. Phys. Lett.* **80**, 2958 (2002).
9. H.W. Schumacher, C. Chappert, R. C. Sousa, P. P. Freitas, and J. Miltat, *Phys. Rev. Lett.* **90**(1) 017204 (2003).
10. C. Chappert, H. Bernas, J. Ferré, V. Kottler, J.P. Jamet, Y. Chen, E. Cambril, T. Devolder, F. Rousseaux, V. Mathet and H. Launois, *Science* **280**, 1919 (1998).
11. J. Miltat, G. Aburquerque and A. Thiaville in *Spin Dynamics in Confined Magnetic Structures*, edited by B. Hillebrands and K. Ounadjela (Springer, Berlin, 2001).
12. M. Bauer et al., *Phys. Rev. B* **61**(5) p3410 (2000)
13. Schumacher et al., *Appl. Phys. Letters* **80**, 3781 (2002)
14. C. Kittel, *Introduction to Solid State Physics*, 5th ed., Wiley, New York, 1976.
15. E. tC. tStoner tand tE. tP. tWohlfarth, Philos. *Trans. R. Soc. London, Ser. A* **240**, 599 (1948)
16. C-R. chang, J-S. Yang, *Phys. Rev. B* **54**(17) pp11957 (1996).
17. "Magnetization precession in confined geometry : physical and numerical aspects". PhD thesis of Gonçalo M. B. Albuquerque, Orsay, July 2002.
18. S. Maat, K. Takano, S.S.P. Parkin, E.E. Fulertton, *Phys. Rev. Lett.* **87**(8), 087202(2001)
19. Wall mobilities in similar Pt/Co systems gave α=0.2. S. Lemerle, private communication.
20. T. Devolder et al., *Appl. Phys. Lett.* **74**, 22, p3383 (1999)
21. S.P. Li, W.S. Lew, J.A.C. Bland, L. Lopez-Diaz, C.A.F Liaz, M. Natali, Y. Chen, Phys. Rev. Lett. **88**(8), 087202 (2002).